

Cross Section for Metastable Production in Low-Energy He^+ -He Collisions*

P. J. MacVicar-Whelan and W. L. Borst[†]

Department of Physics, University of California, Berkeley, California 94720

(Received 30 June 1969)

Metastable He atoms produced by charge exchange of slow He^+ with He were detected by secondary electron emission from a tungsten target. The cross section for metastable production rose from a threshold near 22 eV to a peak value of $2.2 \times 10^{-18} \text{ cm}^2 \pm 50\%$ at 27 eV and decreased to a minimum at 32 eV (center-of-mass energy). A subsequent rise was measured up to 110 eV and was attributed to the increased production of He^m and, to a smaller extent, to kinetic emission of secondary electrons at the higher energies.

I. INTRODUCTION

This paper reports what is probably the first direct measurement of the cross section for the production of metastable atoms in low-energy ion-neutral collisions. The metastables were detected by their ejection of secondary electrons upon striking a tungsten surface. The production of metastables in He ion-neutral collisions at low energies has recently been reported by Utterback.¹ In his case, however, the metastables were indirectly detected by the contribution of the Penning effect to ionization in neutral-neutral collisions. Using a technique similar to that of Utterback, Haugsjaa *et al.*² have recently observed two low-energy resonances in the cross section for metastable Ar formation in Ar^+ -Ar charge transferring collisions.

The structure observed in the present cross section together with the rather high cross-sectional value near threshold indicates the failure of the "adiabatic criterion" as it is usually used.³ Pro-

nounced structure in the excitation functions has also been observed by Dworetzky *et al.*⁴ in the related case of the optical radiation from excited states of He produced in slow He^+ -He collisions. These authors suggested that the reduced energy defect during the collision may cause the low-energy excitation. However, there does not seem to exist an adequate theory yielding the proper shape and value of the cross section near threshold.

II. EXPERIMENTAL DETAILS

Helium ions were produced by an ion gun of the oscillating electron type (Fig. 1) employing an axial magnetic field of about 100 G. The ions were extracted along the electron-path axis through a slit and were focused by an electrostatic-lens system onto the entrance slit of the collision chamber. The axis of the ion gun was displaced from the axis of the rest of the apparatus by about 1 mm. This prevented metastables produced in the ion source from entering the collision chamber. In order to

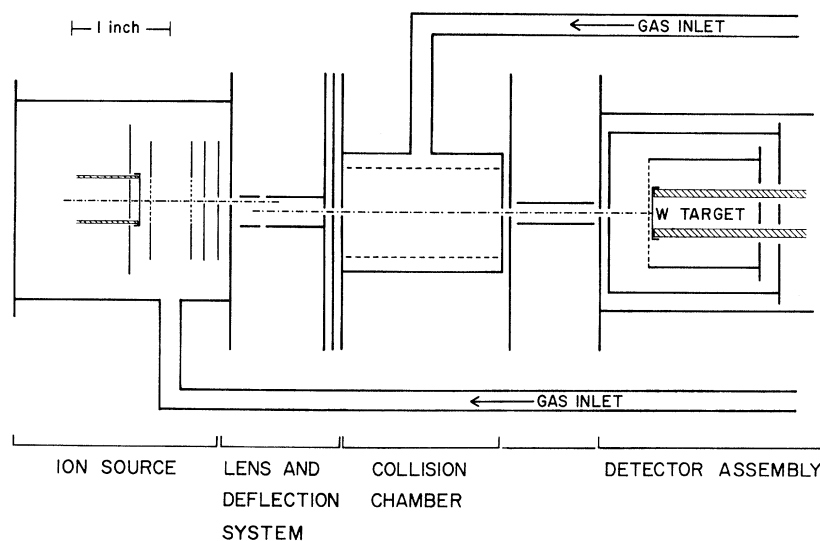


FIG. 1. Schematic of experimental tube (see text). The ion-source axis was displaced from the axis through the other tube elements by 1 mm. The tungsten filaments of the target and ion source were parallel to the slits. In the figure, however, the filaments were rotated by 90° into the plane containing the two axes. The slits were 6 mm long and typically 1 mm wide.

get the ion beam back into the collision chamber, the lens elements were split, and small transverse electric fields were employed for the required deflection. The ion source was operated below the onset for the production of metastable He ions. The neutrals produced in the collision chamber by charge exchange were allowed to enter a detector assembly and impinge upon a tungsten target. The ions in the neutral beam emerging from the collision chamber were removed by deflector plates.

The apparatus was housed in an ultrahigh-vacuum chamber having a base pressure of 6×10^{-10} Torr with all filaments and gauges at the normal operating conditions. The source and the collision chamber were operated at pressures in the 10^{-4} -Torr range. The ion beam into the collision chamber that could produce detectable metastables was determined by maintaining a field-free region between the collision chamber and the tungsten target and by measuring the ion current to the target as a function of collision-chamber pressure. Typical ion currents used were in the 10^{-9} A range. The secondary electron current from the target due to neutrals was then also measured as a function of collision-chamber pressure for each given ion energy (Fig. 2). By taking the slope of the linear signal versus pressure plots as the quantity proportional to the cross section, any contributions from small background currents could be effectively eliminated. Secondary electron currents monitored at the target were typically in the 10^{-14} A range. The grid in the front of the target was biased a few volts positive with respect to the

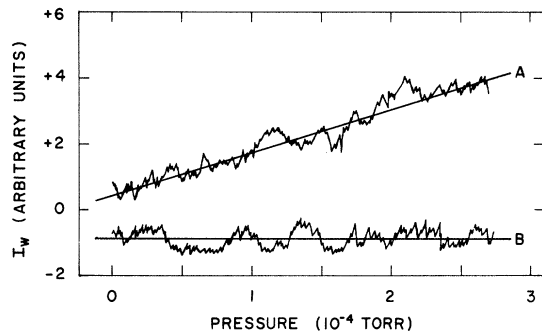


FIG. 2. (a) Retracing of an X-Y recorder plot of secondary electron current leaving the target as a function of collision-chamber pressure at 22.5-eV c.m. energy near threshold. The target current was about 1×10^{-15} A. (b) This curve was obtained when the ion beam was prevented from entering the collision chamber by *not* deflecting it (see Fig. 1). The small zero offset of curve B is due to leakage. At nominal zero pressure there was a small He background in the collision chamber from the ion source. Curves A and B do not intersect because of He^m produced in this background.

target in order to collect all ejected electrons. It was also verified that secondary electron currents were proportional to the ion beam current for an order of magnitude variation in beam current.

Before measurements were made, the target was flashed at 2200 °K to produce an atomically clean surface, as shown by Hagstrum.⁵ The monolayer buildup time was found to be about 15 min. Although it was desirable to make measurements with an atomically clean target immediately after flashing, this was not possible owing to noise currents at the target resulting from the heating. Measurements were obtained within the order of monolayer buildup times.

The secondary electron coefficient γ_i for 160-eV He⁺ ions was found to be 0.13 ± 0.02 . This value is compatible with MacLennan's⁶ value for γ_m of He^m on contaminated tungsten surfaces at thermal energies. It was then assumed that γ_m is equal to the measured γ_i , as shown by Hagstrum.⁷ The energy of the metastables in the present case was assumed to be that of the ions before charge exchange, corrected for the excitation energy of He^m. The ion energy was determined by a retarding potential analysis of the ion beam at the target. The variation of γ_m with energy should have caused an error no larger than about 5%, as shown by Hagstrum.⁸

The pressure in the collision chamber was determined by collecting the slow ions produced in the charge-exchange collisions. These ions were monitored at the grid in the collision chamber (see Fig. 1), which for this measurement was biased a few volts negative with respect to the collision chamber walls in order to give a saturated ion current. The pressure could also be obtained from the measured pressure in the surrounding vessel together with the conductance of the collision-chamber slits. Furthermore, the pressure was calculated from the measured pressure at the gas-input line. The uncertainty in collision-chamber pressure was about 30%.

III. RESULTS AND DISCUSSION

The measurements are shown in Fig. 3. It is noted at He^m, atoms appear in measurable amounts around 22-eV c.m. energy. The cross section rises to a peak at about 27 eV, starts to decline, and rises again at about 32 eV. The cross section at the peak was found to be 2.2×10^{-18} cm² \pm 50%, the error being mainly due to uncertainties in pressure and γ_m .

The inception of the rise to the peak and the location of the peak, as well as the incipient decline, parallel the observations of Utterback¹ obtained in a different fashion. Utterback produced a He neutral beam containing He^m by charge exchange of He⁺ with He and detected the He^m atoms by the contribution of the Penning effect to ionizing

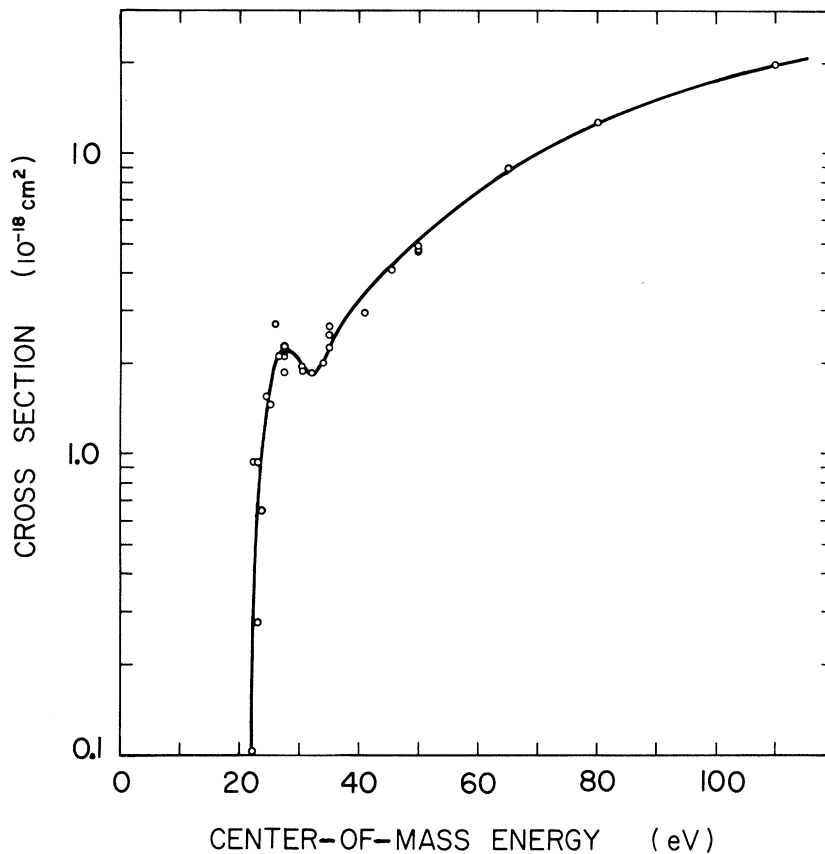


FIG. 3. Cross section for the production of metastable He atoms by impact of slow He^+ ions on He as a function of c.m. energy. The cross section refers to metastables scattered into a half angle of about 5° in the forward direction.

He- H_2 collisions. The cross section for total negative-charge production in these collisions exhibited structure at low energies. In contrast to this, the corresponding cross section for a H_2 beam on He did not show structure. The difference of these two cross sections yielded a curve rising at about 23 eV, peaking near 28 eV, and declining to about 33 eV in the He-He c.m. system. This difference curve was proportional to the cross section for the production of He^m by charge exchange. It was estimated that the results could have been achieved by a fraction of 0.3% He^m in the neutral beam. We obtain a fraction of about 0.2% He^m for the peak in Fig. 2.

Utterback's difference curve does not extend beyond 33 eV and does not indicate the later rise observed in the present work. However, in plotting the H_2 -He data, footnote 6 of Ref. 1 states, "All actual data points for H_2 -He have been arbitrarily raised 30% so that the He- H_2 and H_2 -He curves coincide above the structure." Had this not been done, the He-He difference curve plotted would have paralleled the present curve and shown a new rise near 33 eV. If the Penning ionization cross section were constant with bombarding particle energy, then our curve should agree in relative shape with the difference in the two cross sections measured by Utterback, without applying the

30% correction for the H_2 -He curve. The actually observed lack of agreement gives a decrease of the Penning ionization cross section with energy of about 0.6%/V (at least from 66 to 110 eV in the laboratory system) provided that this disagreement is indeed due to only this variation. Hollstein *et al.*⁹ found a somewhat smaller decrease of about 0.1% for He^m in N_2 and He^m in Ar.

The increase of metastables beyond the peak beginning at about 32 eV may be accounted for by the work of Dworetzky *et al.*,⁴ from which it follows that at about this energy, excitation of many higher-lying states occurs. These states may contribute to the observed target current by cascading to He^m . On the other hand, photons from radiatively decaying states in the charge-exchange chamber are emitted in all directions and very few would reach the target. Hence, any photoelectron contribution to the target current is believed to be negligible. However, since excited (as well as unexcited) neutrals are scattered predominantly in the forward direction, any increase in He^m by cascading would be included in the neutral current and be measured.

Retarding potential curves (Fig. 4) of the emitted secondary electrons were taken at 27 eV, corresponding to the peak in Fig. 3, and at 64 eV. Both curves were similar in shape and paralleled those

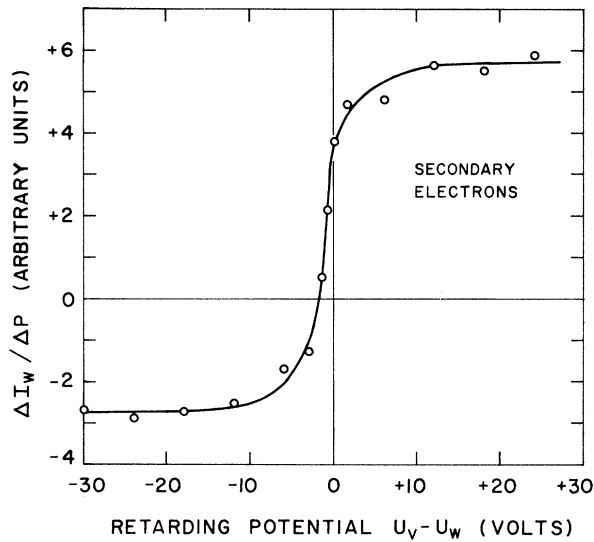


FIG. 4. Typical retarding potential curve of target current (actually of slope of target current as obtained from plots similar to Fig. 2) as a function of voltage between grid V and target W . The curve shown was taken at 64-eV c.m. energy. For positive potentials, the observed current is due to secondary electrons leaving the target, whereas the negative current observed for negative potentials was ascribed to positive ions leaving the target.

obtained by Greene¹⁰ for He^m on contaminated surfaces. Determination of the energy distribution of the ejected electrons was rendered difficult since, as the potential of the grid in front of the target passed through zero and became negative, the target current changed sign from positive to negative values. This negative current, which can be ascribed to positive ions leaving the target, saturated at about $\frac{1}{5}$ to $\frac{1}{2}$ of the (positive) secondary electron current. Both positive and negative target currents were proportional to collision-chamber pressure and ion-beam current. The potentials applied to the electrodes of the target assembly were chosen so as to prevent any charged particles from entering the target space. Any currents measured at the target must have originated

at the target. Secondary electron ejection from the grid in front of the target was negligible as the grid transparency was 90%, and it was outgassed periodically by electron bombardment from the target.

For reasons given above, the emission of positive ions was attributed to bombardment of the target by He and/or He^m . It is possible that the 45–220-eV neutrals on the laboratory scale could sputter off positive ions from the target, but the magnitude of the positive-ion current seemed too great for such a source. Another possible explanation is that of surface ionization of He^m atoms by the contaminated target. Such an effect has been noted by Varney¹¹ for Ar^m and N_2^m .

The present measurements extend to an energy of 220 eV in the laboratory system. Data taken at higher energies indicated the onset of kinetic emission of secondary electrons by ground-state neutrals. This increases the apparent cross section. Unfortunately, little information exists on the secondary electron yield γ_{kin} for kinetic emission from clean or only slightly contaminated surfaces. The only work we are aware of that corresponds to our experimental conditions is that of Waters¹² for Li^+ ions on atomically clean as well as N_2 and O_2 contaminated tungsten surfaces. From this work it is estimated that, at a laboratory energy of 200 eV, $\gamma_{\text{kin}} \approx 1 \times 10^{-4}$ for He^+ on atomically clean tungsten, and $\gamma_{\text{kin}} \approx 2 \times 10^{-3}$ for tungsten covered with a monolayer of nitrogen. The first value makes the contribution to the cross section in Fig. 3 by kinetically ejected electrons negligible. The latter value introduces a contribution to the cross section at the higher energies in Fig. 3. We feel, however, that the general shape of the cross section much below 50-eV c.m. energy should be preserved, since γ_{kin} decreases rapidly below such energies. In particular, the resonance observed at 27 eV should be undistorted.

ACKNOWLEDGMENTS

We wish to acknowledge our thanks to Dr. R. N. Varney for his valuable discussions, and to Professor L. B. Loeb under whose supervision this work was carried out. Thanks are also due to the Office of Naval Research for the support of this project.

*Work supported by a grant from the U. S. Office of Naval Research.

†Present address: Department of Physics, University of Pittsburgh, Pittsburgh, Pa. 15213.

¹N. G. Utterback, Phys. Rev. Letters **12**, 295 (1964).

²P. O. Haugsjaa, R. C. Amme, and N. G. Utterback, Phys. Rev. Letters **22**, 322 (1969).

³H. S. W. Massey and E. H. S. Burhop, *Electronic and Ionic Impact Phenomena* (Clarendon Press, Oxford,

England, 1952).

⁴S. Dworetzky, R. Novick, W. W. Smith, and N. Tolk, Phys. Rev. Letters **18**, 939 (1967).

⁵H. D. Hagstrum, Phys. Rev. **96**, 325 (1954).

⁶D. A. MacLennan, Phys. Rev. **148**, 218 (1966).

⁷H. D. Hagstrum, J. Appl. Phys. **31**, 897 (1960).

⁸H. D. Hagstrum, Phys. Rev. **104**, 1516 (1956).

⁹M. Hollstein, D. C. Lorents, J. R. Peterson, and R. A. Young (private communication).

¹⁰D. Greene, Proc. Phys. Soc. (London) **B63**, 876 (1950).

¹¹R. N. Varney, Phys. Rev. **157**, 113 (1967); **157**, 116

(1967); **175**, 98 (1968).

¹²P. M. Waters, Phys. Rev. **111**, 1053 (1958).

Effects of Coulomb Interactions on the Landau Diamagnetism*

A. Isihara[†]

Solid State Science Division, Argonne National Laboratory, Argonne, Illinois 60439

and

M. Wadati

Statistical Physics Laboratory,

Department of Physics and Astronomy, State University of New York, Buffalo, New York

(Received 18 August 1969)

The diamagnetic susceptibility of an electron gas is reduced by Coulomb interactions below the Landau value in proportion to $\epsilon\beta\kappa_0^2$, where ϵ is the plasma parameter, κ_0 is the Debye screening constant, and $\beta = 1/kT$.

1. INTRODUCTION

According to Van Leeuwen's theorem, there are no magnetic-field effects on the statistical properties of a classical electron gas. However, Landau proved the existence of diamagnetism even if the electrons obey the classical Boltzmann statistics. The diamagnetic susceptibility is just one-third of the spin paramagnetic susceptibility and is given by

$$\chi = -\frac{1}{3}n\beta(\hbar e/4\pi mc)^2. \quad (1.1)$$

The Landau diamagnetism is due to the quantized energy levels:

$$E_n = (n + \frac{1}{2})e\hbar H/mc + p_z^2/2m. \quad (1.2)$$

As one can see from Eq. (1.1), it vanishes in the limit $\hbar \rightarrow 0$. Therefore, there is no conflict between the Van Leeuwen theorem and the diamagnetism.

The Landau diamagnetism is derived for free electrons. If the motion of electrons in the quantized energy levels is the cause for the diamagnetism one might expect that the susceptibility will probably be reduced if the Coulomb interactions are introduced. It is the purpose of this paper to report that this reduction is indeed the case. In addition, we shall present a relation for the fugacity which improves the one used in the previous paper.¹

For our purpose, we shall evaluate the grand partition function to order ϵ^2 , where ϵ is the plasma parameter defined by

$$\epsilon = 2\pi^{1/2}n^{1/2}\beta^{3/2}e^3. \quad (1.3)$$

It is of course desirable to develop the theory completely generally, but the problem is very difficult, and a perturbation method is used. Once the grand partition function Ξ is obtained, the susceptibility is evaluated from the relation

$$\chi = \frac{1}{H} \left(\frac{\partial \ln \Xi}{\partial H} \right)_{H=0}, \quad (1.4)$$

where the differentiation is performed at constant fugacity Z .

We shall take the units in this paper such that $\hbar = 1$ and $2m = 1$, where m is the electron mass. In these units the Landau susceptibility given by Eq. (1.1) becomes

$$\chi = -\frac{1}{3}n\beta(e/c)^2. \quad (1.5)$$

As usual, the ions are smeared out to form a cloud of positive charges.

2. GRAND PARTITION FUNCTION

The grand partition function in the ring-diagram approximation has been given by the formula²